Local lamellar organisation of discotic mesogens carrying fluorinated tails†‡

Paul H. J. Kouwer,§[a] Stephen J. Picken[b] and Georg H. Mehl*[a]

Received 25th May 2007, Accepted 24th July 2007
First published as an Advance Article on the web 9th August 2007
DOI: 10.1039/b707880c

A series of disc-shaped liquid crystals, monomers and dimers, have been investigated. A spacer linked to the pentakis(phenylethynyl)phenoxy core of the mesogens was substituted with perfluorinated chains to investigate the microphase segregating effect of such groups. The nematic phase, commonly found for these mesogens, is strongly stabilised by the presence of the fluorinated groups. X-Ray diffraction studies indicate clearly the onset of nanophase segregation in the nematic phase. Remarkable is the result, that the nanophase segregation directs the systems towards a *lamellar* organisation, rather than the columnar order that is commonly found for disc-shaped mesogens. This is also confirmed by the order in the underlying crystalline phase. X-Ray diffraction studies of the nematic phase show the characteristics of cybotactic smectic clustering, which has not been observed for discotic systems so far.

Introduction

The combination of order and fluidity that liquid crystals offer is the basis of today's multi-billion dollar display industry. Nearly all commercial display applications employ liquid crystals in their lowest ordered phase, the nematic phase. In this phase, the mesogens possess solely long-range orientational order and lack positional order. Hence, characteristic X-ray diffraction (XRD) patterns of nematics show only two diffuse reflections. For rod-shaped liquid crystals, the small angle reflection corresponds to the length (long axis) of the mesogen, while the wide angle reflection correlates to the mesogens short axes. Analogously for discotic liquid crystals, the small and wide angle reflections relate to the diameter and the ''thickness'' of the disc-shaped mesogen, respectively.[1]

However, a range of low molar mass liquid crystals as well as polymers show splitting up of the diffuse scattering pattern in the small angle region in a manner typically found for the SmC phase. For low molar mass nematic systems, a deviation in the molecular structure from the classical cylinder symmetry or, alternatively, the inclusion of microphase separating groups favours the formation of these local smectic-like correlations. For polymers either a minimum degree of polymerization or dendritic structure seems to be required.[2] Recently, the observation of split small angle reflections has been discussed for bent-core molecules as further experimental evidence for the formation a biaxial nematic phase.[3]

To combine the typical nematic behaviour observed by different experimental techniques (optical polarizing microscopy, miscibility studies, dielectric spectroscopy) and the smectic-like fluctuations (short-range positional order) in these systems, the term *cybotactic nematic* has been used. The difficulty to reconcile this nomenclature with the classical picture of the nematic phase was realized early on and this effect is usually viewed in the context of pre-transitional behaviour preceding a smectic phase.[4] Despite this, cybotactic behaviour over a wide temperature range has been reported as well, in fact, some are observed over the entire nematic phase.[4a] Noticeable is that cybotactic structuring has not yet been reported for discotic liquid crystal systems,[5] though the formation of smectic phases has been realized recently for suitably modified disc-shaped molecules[6] or dyads containing disc-shaped and rod-shaped moieties.[7]

In this contribution, we will discuss the role of a single attached perfluorinated chain on the phase behaviour of a disc-shaped nematogen, including the formation of *smectic*-like fluctuations in the discotic nematic phase. As the mesogenic moiety the pentakis(phenylethynyl)phenoxy group was chosen (see Scheme 1), as this mesogen is relatively easy functionalised and shows a nematic phase over a wide temperature range. The disc is functionalised with a flexible hydrocarbon tail and at the terminal end of the tail a perfluorinated spacer or tail is attached. Fluorocarbons are well-known for their strong microphase segregation effect with hydrocarbons. This property has been utilised to its full effect in rod-shaped liquid crystals.[8] Similar strongly stabilising effects are observed when dimethylsiloxane groups[9] or ionic groups[10] are introduced. Examples of the use of such strong directing groups in discotic mesogens are very limited.[11]

[a]*University of Hull, Department of Chemistry, Cottingham Road, Hull, UK HU6 7RX. E-mail: g.h.mehl@hull.ac.uk; Fax: +44 1482 466411*
[b]*Delft University of Technology, Polymer Materials and Engineering, Julianalaan 136, 2628 BL Delft, The Netherlands. E-mail: s.j.picken@tnw.tudelft.nl; Fax: +31 15 2784715*

† Electronic supplementary information (ESI) available: avi movie on miscibility of **3a** and **3b**. See DOI: 10.1039/b707880c

‡ The HTML version of this article has been enhanced with colour images.

§ Current address: Radboud University, IMM, Toernooiveld 1, 6525 ED Nijmegen, The Netherlands. E-mail: p.kouwer@science.ru.nl

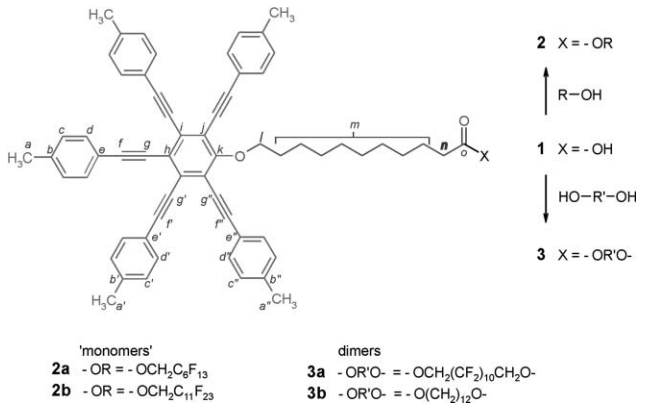

Scheme 1 Monomers **2** and dimers **3** were prepared *via* an esterification reaction: ROH or R′(OH)$_2$, **1**, DIC, DMAP and *p*-TSA in CH_2Cl_2, 5 d at room temperature.

Results and discussion

Synthesis

The investigated mesogens were prepared by a *N*,*N*′-diisopropylcarbodiimide (DIC) mediated esterification of the disc-shaped mesogen **1** with the appropriate alcohols or diols, catalyzed by 4-(dimethylamino)pyridine (DMAP) and *para*-toluenesulfonic acid (*p*-TSA), similar to literature procedures, see Scheme 1.[12] Column chromatography over SiO_2 and subsequent crystallization from CH_2Cl_2–methanol mixtures yielded products in moderate to good yields. The monomers and dimers were characterized by ^{1}H, ^{13}C and ^{19}F NMR spectroscopy, MALDI-ToF mass spectroscopy and elemental analysis.

Mesophase behaviour

The liquid crystalline properties of the mesogens were investigated using optical polarizing microscopy (OPM) and differential scanning calorimetry (DSC). The results are summarized in Table 1.

All synthesised materials show a nematic phase at elevated temperatures with low viscous *schlieren* and marbled optical textures. Other derivatives based on the same mesogenic moiety as **2** and **3** show similar characteristics.[12] Typically, the entropy changes at the nematic to isotropic transition are very small ($\leqslant$0.5 J mol^{-1} K^{-1}). In the nematic and the isotropic phases, the fluorinated materials **2a**, **b** and **3a** are completely miscible with the alkyl equivalent **3b**. Fig. 1 shows polarizing microscopy images of a contact sample of **3b** (with the bulk in the top, left corner of the image) and **3a** (bulk to the right). At 183 °C (Fig. 2a), the bulk of **3b** is still isotropic, while for **3a** with a higher clearing temperature, a marbled texture is observed. Upon cooling, first **3b** turns nematic and gradually the isotropic area at the interface decreases in size (Figs. 1b and 1c). At 180 °C the entire sample shows a homogeneously mixed nematic texture, suggesting full miscibility between the two compounds. The ESI contains a short movie that clearly demonstrates the miscibility between the semifluorinated and the hydrocarbon dimer, by cooling the contact sample from 185 to 179 °C (cooling rate 5 °C min^{-1}).†

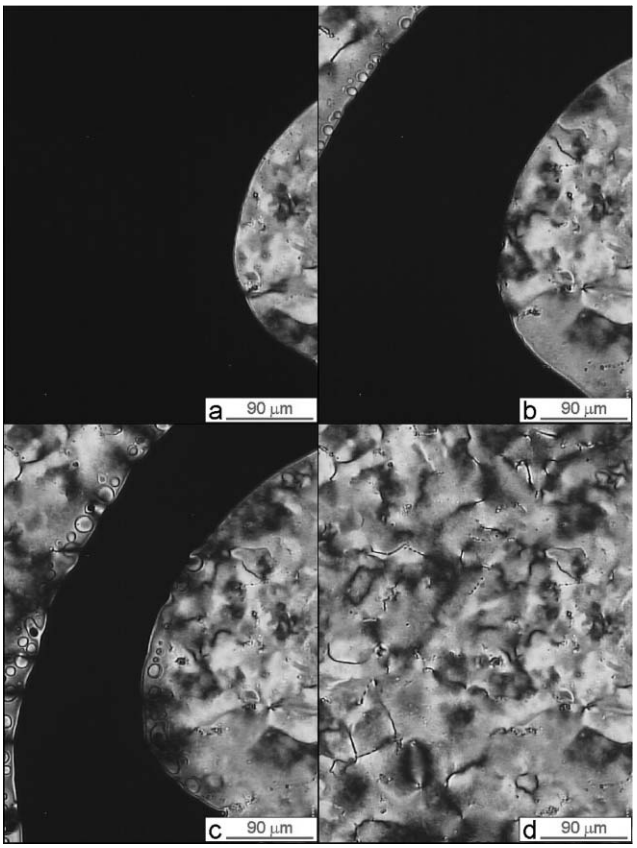

Fig. 1 Optical microscopy pictures of a contact sample of **3a** (left, top) and **3b** (right) at (a) 183 °C; (b) 182 °C; (c) 181 °C and (d) 180 °C. Pictures are taken at exactly the same spot in the sample (between crossed polarizers). The cooling rate was 5 °C min^{-1} and the sample was not annealed before the pictures were taken. A short movie, included in the ESI, clearly shows the miscibility between the two compounds.†

The liquid crystalline properties of the fluorinated mesogens **2a**, **2b** and **3a** were compared to those of analogues with the

Table 1 Liquid crystalline properties of the investigated mesogens

Mesogen	ϕ_{rigid}[a]	Phase behaviour[b,c]							$\Delta S_{NI}/n$[d]/J mol^{-1} K^{-1}
2a	0.647	Cr_1	155 (12)	Cr_2	165 (26)	N	176 (0.18)	I	0.40
2b	0.575	Cr_1	164 (11)	Cr_2	181 (26)	N	192 (0.26)	I	0.56
3a	0.670	Cr			166 (28)	N	196 (0.41)	I	0.44
3b	0.712	Cr			159 (34)	N	183 (0.38)	I	0.42
3a + **3b**[e]	0.690	Cr				N	180 (0.39)	I	0.43

[a] The volume fraction of the rigid mesogens ϕ_{rigid} is defined in the text. [b] Phase transitions in °C and latent heat values (in brackets) in kJ mol^{-1}. [c] Abbreviations: Cr, Cr_1, Cr_2 = crystal phases; N = nematic; I = isotropic. [d] Entropy change at the nematic to isotropic phase transition per mesogenic group (*n*). [e] Equimolar mixture.

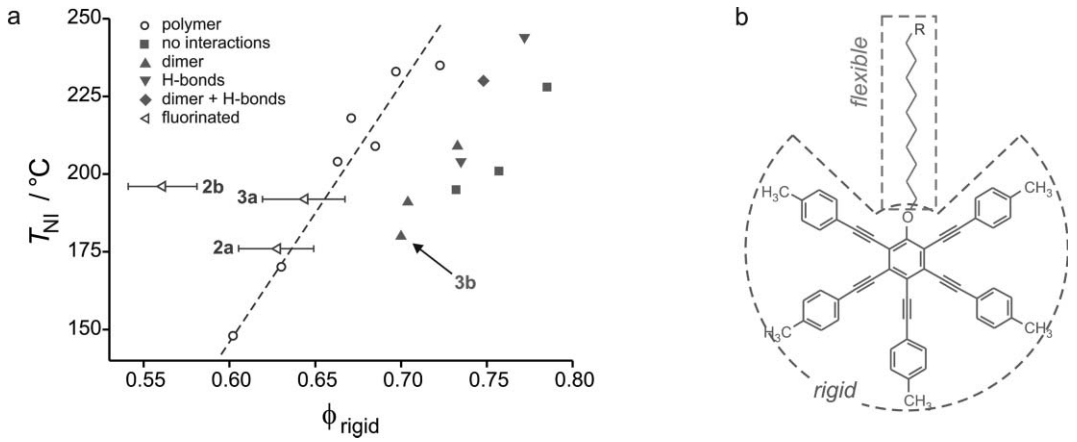

Fig. 2 T_{NI} (T_{NI}: nematic to isotropic transition) as a function of rigid mesogen fraction ϕ_{rigid} for differently substituted discotic mesogens: (○) polymers (copolymers with various degrees of substitution to the polyacrylate backbone),[12] the solid figures represent different low molar mass species: (■) no specific additional interactions; (▲) dimers; (▼) stabilisation by hydrogen bonding and (◆) dimers with H bond stabilisation. The fluorinated materials **2a**, **2b** and **3a** discussed in this paper are shown with a ◁. (b) Generic structure of studied disc-shaped mesogens; R groups include a polyacrylate backbone and (bifunctional) esters and amides with a variety of substituents, such as alkyl, oligoglycol and crown ether moieties.[12,14]

same mesogenic core, but different terminal substituents (see Fig. 2b with various R groups).[12] Previous research has shown a clear relation between the weight-based rigid mesogen fraction (M) and the clearing temperature.[13,14] But since the volumes as well as the thermal expansion coefficients of hydrocarbon and fluorocarbon groups are very different, this mass fraction-based method could not be applied for **2** and **3a**. In addition, we were unable to experimentally measure the densities of the compounds at the temperatures of interest (>150 °C).

Therefore, we estimated the partial volumes of the CH_2 and CF_2 groups in the mesogens using literature values of their respective thermal expansion coefficients that were recently published for disc-shaped liquid crystals.[6a] An extra 10% error in the determined values for the rigid mesogen volume fraction, indicated by the error bars in Fig. 2a, was added to cover further uncertainties arising from the above method.

Fig. 2a shows the linear relation between the clearing temperature and the volume fraction ϕ_{rigid} for a series of side chain polymers.[14a] As expected, low molecular mass materials show lower clearing temperatures since the stabilising effect of the polymer backbone is lost. Specific interactions such as hydrogen bonding and dimerisation of mesogens tend to restabilise the nematic phase. The introduction of an intermediately long fluorinated tail (**2a** and **3a**), however, stabilises the nematic phase up to the level of the polymeric species. A further increase in the length of the fluorinated chain shows the same clearing temperature at much lower rigid mesogen fraction.

Despite the fact that Fig. 2a uses estimated values for the rigid mesogen fraction, it is evident that the nematic phases displayed by **2a**, **3a** and in particular by **2b** are strongly stabilised. The combination of this result with the DSC and OPM studies that support the formation of common nematic phases prompted us to investigate the mesophase organisation further using X-ray diffraction (XRD) techniques.

X-Ray diffraction studies

Mesogen **3b**, without any fluorinated groups, shows the characteristic diffraction pattern of a (discotic) nematic liquid crystal, characterized by two diffuse halos, see Fig. 3 (bottom curve). Reflection B is attributed to the average lateral disc–disc distance in the sample (~15 Å), whereas the second diffuse halo D is assigned to the face-on disc–disc distance between the mesogens (~4 Å), superposed with the average distance between the alkyl groups from the spacer (~4.5 Å).[12]

The diffraction pattern of analogue **3a**, with ten CF_2 groups placed in the spacer is remarkably different, despite all the similarities found in OPM and DSC studies, see Fig. 4. Two extra reflections are observed: A and C. Weak alignment of the dimer in the magnetic field allowed us to investigate the orientation of the reflections A–D with respect to the field (Fig. 4a). As expected for the discotic mesogen (with a negative

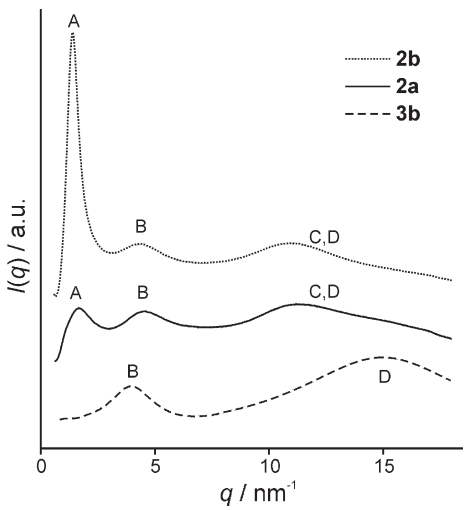

Fig. 3 Radially integrated diffraction patterns of **2b** (top); **2a** (middle) and **3b** (bottom). As none of these samples aligned in the magnetic field, no 2D diffractograms are shown.

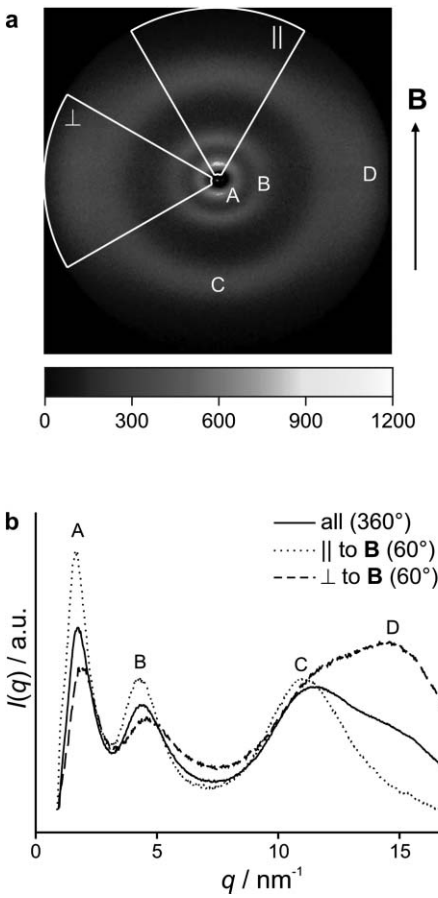

Fig. 4 XRD results of mesogen **3a** in the nematic phase at $T = 172$ °C: (a) 2D diffractogram, partly aligned by the magnetic field; and (b) radially integrated patterns. To distinguish individual broad reflections, the pattern has been integrated over 360° (—), over 60° parallel to the magnetic field (···) and over 60° perpendicular to the magnetic field (---). The integration limits are indicated by the arcs in a. The letters in a and b refer to the reflections that are further discussed in the text.

magnetic susceptibility), reflection B is parallel to the field, while D is perpendicular. Reflection A is also parallel and, interestingly, C shows no preferred orientation towards the magnetic field. The difference in alignment of these diffuse diffraction peaks is best visualised by partial integration along and perpendicular to the magnetic field, see Fig. 4b.

Reflection C is assigned to the lateral spacing between two neighbouring fluorinated alkyl groups, typically observed at 5.5–6 Å, as the fluorinated alkyl groups are slightly more voluminous than their non-fluorinated counterparts.[8] The separate observation of reflections C and D (both in position and orientation) is a strong indication for microphase segregation of the fluorinated alkyl groups from the rest of the mesogen. Further evidence for microphase segregation is provided by spacing A, observed at 35 Å, *i.e.* at much larger distances than the diameter of the discotic moiety. This extra small angle reflection can be explained by considering a (locally) microphase segregated structure, where A represents the average distance between the separated layers. The relatively large half-width of A shows that the layering is strictly short-range, and therefore, the structure corresponds better to a SmA cybotactic nematic than to a ordinary smectic phase.

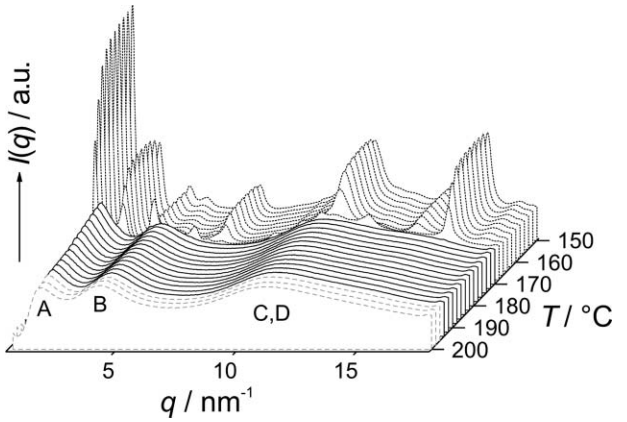

Fig. 5 Radially integrated X-ray diffraction patterns of **3a** at different temperatures (isotropic: short dash, nematic: full lines, crystalline: dotted). Note that reflections A and C also show up in the isotropic phase.

Fig. 5 shows the integrated diffraction patterns of **3a** in the crystalline, nematic and isotropic phases between 150 and 200 °C. The small angle reflection A is also present in the isotropic phase. This indicates that the microphase separated structure already exists in the isotropic phase and, therefore, can be traced back to the phase segregating forces of the fluorocarbon and the hydrocarbon groups. This mechanism of nanophase segregation is different from the shape-induced phase segregation in the linked disc–rod system that we presented before.[7,15] In these systems, the different groups were homogeneously mixed in the isotropic and the nematic phase and the small angle reflection indicating phase segregation was only observed after the transition into one of the smectic phases.

The crystalline phase shows a set of sharp small and wide angle reflections. The small angle area shows a clear layered pattern with a corresponding layer spacing of 50.5 Å. The large intermediately sharp reflection at 5.5 Å indicates close packing of the fluorocarbon groups. The second sharp reflection in the wide angle area is observed at 3.9 Å. This reflection corresponds to the face-on distance between two adjacent discotic moieties. The observation of these basic reflections and the absence of cross reflections suggests the formation of a soft crystal phase with a well-defined columnar structure, perpendicular to the lamellar organisation (similar to that observed in columnar lamellar Col_L phases). In this model, a face-to-face disc–disc distance of 3.9 Å is relatively large, compared to other columnar systems.[5] This larger value may be explained by a small tilt of the discs with respect to the formed column axis.

The layered pattern observed is even more pronounced in the soft crystal phase of **2b**, with an increased fluorinated tail length compared to **3a**, see Fig. 6. The (001) to (005) reflections of the lamellar structure are clearly visible and give a layer spacing of 53.2 Å. In addition, between the (003) and (004) reflection a rather diffuse peak is observed, see the inset in Fig. 6. Its spacing, obtained after fitting the reflection to a Gaussian distribution is 14.1 Å, which corresponds roughly to the width a disc.[7b] The presence of this reflection supports the model of the Col_L-like soft crystal phase discussed above.

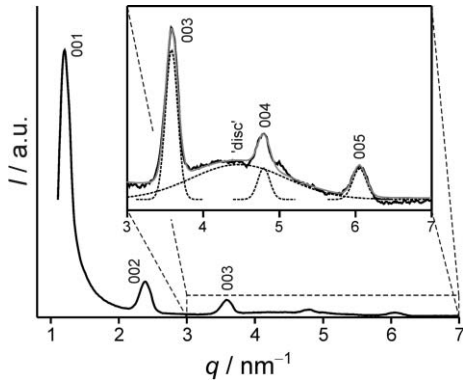

Fig. 6 Small angle area of the integrated diffraction pattern of **2b** in the crystalline phase (Cr_2, 175 °C). The inset shows a magnification, highlighting the broad diffraction peak from the width of the discs (dotted lines are Gaussian fits to the experimental data, the solid curve is the sum of the fits (including the 001 and 002 reflection).

In the nematic phase, the fluorinated mesogens **2a**, **b** and **3a** also show very similar behaviour in the X-ray diffraction experiments. In fact, the diffraction patterns of the three fluorinated materials in this study are nearly identical, apart from the position and intensity of the layer spacing A,[16] see also traces in Fig. 3 and 4. Quantitative results, summarized in Table 2, were obtained after fitting the radially integrated spectra to Lorentzian distributions. The differences in *d*-spacings for **2a**, **2b** and **3a** can be attributed solely to the length of the fluorinated tail or spacer: 2 × C_6F_{13}, 2 × $C_{11}F_{23}$ and $C_{10}F_{20}$, respectively. The results indicate that the layers separate 0.6–0.7 Å per CF_2 unit, which in turn suggests a high degree of disorder of the perfluorinated units. This is consistent with their isotropic appearance in the aligned XRD experiments of **3a**.

To further investigate the induced cybotactic layering, an excess of discs was introduced into the microphase segregated structure by mixing **3a** with **3b** in equimolar quantities. X-Ray diffraction studies on the sample showed that reflection A broadens and shifts to smaller angles, illustrating a larger spaced layer formation, however, with a decreased correlation length. The nearly 50 Å spacing observed for the sample fits to the original 35 Å for **3a** and an extra 15 Å that matches the dimensions of a second disc, pointing towards an average structure of *two* layers of discs in between the fluorinated spacers. It is anticipated that additional amounts of discs will be positioned into the discotic layers, slowly driving the fluorinated layers apart, thereby destroying the cybotactic organisation.

Table 2 X-Ray diffraction data and the experimental and calculated values of the molecular volume for the investigated compounds in the N phase

		Spacings/Å			
Mesogen	*T*/°C	A	B	C	D
2a	172	36.3	14.1	5.7	4.3
2b	182	43.9	14.2	5.7	4.2
3a	172	35.2	14.1	5.6	4.3
3b	172	—	15.4	—	4.2
3a + **3b**[a]	172	49.6	14.6	5.6	4.3

[a] Equimolar mixture.

Table 3 Relative correlation lengths (ξ/d) of the reflections A and B in the N phase

		Reflection A			Reflection B		
Mesogen	*T*/°C	*d*/Å	ξ/Å	ξ/d	*d*/Å	ξ/Å	ξ/d
2a	172	36.3	116	3.2	14.1	47	3.3
2b	182	43.9	273	6.2	14.2	48	3.3
3a	172	35.2	104	3.0	14.1	48	3.4
3b	172	—	—	—	15.4	56	3.6
3a + **3b**[a]	172	49.6	122	2.5	14.6	50	3.4

[a] Equimolar mixture.

From the half-widths of the Lorentzian distribution functions, information can be obtained on the correlation length ξ, representing the extent of (short-range) positional order in a low ordered mesophase. Dividing ξ by the spacing *d*, obtained from applying Bragg's Law, gives a measure for the order in terms of *number of mesogens*, suitable to mutually compare the order in a series of similar materials.

The relative correlation length (ξ/d) has been calculated for reflections A and B of mesogens **2** and **3** and the mixture **3a** + **3b**, see Table 3. For reflection B, the relative correlation length is nearly identical for all compounds. This indicates that the mesogenic order (*i.e.* the correlative organisation of the discs) in these materials is very similar. The values observed for reflection A are more different. The mixture **3a** + **3b**, wherein the influence of the fluorinated groups is diluted the most, shows the lowest relative correlation length. Compounds **2a** and **3a**, with similar amounts of fluorinated chains, show very similar values and, clearly, the extent of order in **2b** is the highest. In other words, the number of fluorinated groups in this series dictates the extent of order in the cybotactic cluster. This has implications for the further design of nanophase segregated structures. In the design of complex hierarchal structures, volume fractions as well as geometrical factors need to be carefully considered.

From the experimental data, it can be concluded that through further optimisation of the interactions of the fluorinated tails, higher ordered phases, such as smectic phases for discotic mesogens, could be feasible. Alternatively, a modulation of the interactions leading to a *reduction* of the ordering could result in relative correlation lengths of the order of the molecular dimensions of the systems. This would bring these systems in line with the observations found for the formation of biaxial nematic phase behaviour in bent-core molecules and allow the investigation of the relationship between biaxiality and smectic clustering.[3b]

Conclusions

In conclusion, we have prepared and investigated the mesomorphic behaviour of a series of discotic liquid crystals bearing partly fluorinated chains. The fluorocarbon chains induce nanophase segregation, which in turn thermally stabilises the mesophase. The nanophase segregation has the character of smectic A-like fluctuations. To the best of our knowledge, such smectic fluctuations, or in fact any

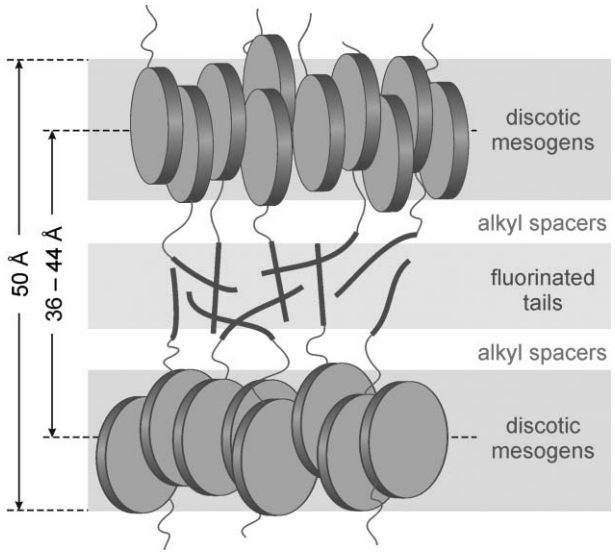

Fig. 7 Schematic representation of the cybotactic nematic mesophase of **2a** and **2b**, wherein layers of nematically ordered discs are (locally) separated ~40 Å by layers of fluorinated tails. An analogous picture for dimer **3a** can be drawn (where the fluorinated tails transform into spacers). The mixture of **3a** and **3b** shows two layers of discs separated by a ~50 Å single layer of fluorinated spacers.

fluctuations, have not been observed in discotic systems before. The associated layering is only short-range and the mesogens show an ordinary nematic phase, which means that they are miscible with other (discotic) liquid crystals in the nematic phase. A schematic representation of the local organisation of the fluorinated materials is shown in Fig. 7. The director of the discotic mesogens is aligned in a plane perpendicular to the magnetic field (pointing up along the layer normal). The average distance between two adjacent layers of (nematically ordered) discs, separated by soft layers of fluorinated tails, can be tuned by changing the length of the fluorinated group or the concentration of discs in the system. It is anticipated that by optimising the cross sections between the discs and the fluorinated tails, long-range smectic order with disc-shaped mesogens can be achieved. Alternatively it could allow for the investigation of the correlation between nematic biaxiality and cybotactic clustering.

Experimental

General

Mesogen **1** was prepared according to literature procedures.[12] The other materials were used as purchased unless stated otherwise. Solvents were used as received. The fluorinated tails and spacers were obtained from Lancaster UK ($HOCH_2C_{11}F_{23}$ and $HOCH_2C_{10}F_{20}CH_2OH$) and Fluorochem ($HOCH_2C_6F_{13}$).

Instrumental

NMR spectra were recorded on a Jeol JNM-ECP 400 FT-IR spectrometer (400 MHz). Chemical shifts are reported in ppm relative to TMS. Mass spectra were obtained on a Bruker Reflex IV MALDI-ToF Mass Spectrometer, operating in a reflection mode. The samples were mixed with the matrix material 2-(4-hydoxyphenylazo)benzoic acid (solution in CH_2Cl_2). To obtain reliable data the results of 100–200 laser shots, taken at 10–20 different places in the samples were averaged. Phase transitions were determined using a Perkin Elmer DSC 7 in a nitrogen atmosphere against an indium standard (reported temperatures are the onset of the endotherm). The mesophases were studied on an Olympus BH-2 optical polarizing microscope, equipped with a Mettler FP82 HT hot stage with a Mettler FP90 central processor and a JVC digital video camera for picture capturing. XRD experiments were performed on a MAR345 diffractometer with a 2D image plate detector (Cu Kα radiation, graphite monochromator, λ = 1.54 Å). The samples were heated in the presence of a magnetic field using a home-built capillary furnace. Spacings were calculated by applying Bragg's Law: $2d\sin\theta = n\lambda$, where d is the spacing, θ is half the diffraction angle, n is an integer and λ is the wavelength (λ = 1.54 Å). Integrated diffractograms are shown as a function of the modulus of the scattering vector: $q \equiv 2\pi n/d = 4\pi\sin\theta/\lambda$. The correlation lengths ξ are calculated after fitting the reflections with Lorentzian curves and determining the half-width at half maximum (HWHM) of the reflection. The Scherrer equation $\xi = 2\pi/\Delta q$ gives the correlation length, with Δq being the HWHM of the reflection in reciprocal space.

Synthesis

General procedure for esterifications. A solution of the appropriate alcohol (0.11 mmol) or diol (0.045 mmol), mesogen **1** (0.1 mmol), *N*,*N*′-diisopropylcarbodiimide (DIC, 5 mmol), 4-(dimethylamino)pyridine (DMAP, 50 μmol) and *para*-toluenesulfonic acid (*p*-TSA, 50 μmol) was stirred in CH_2Cl_2 (10 mL) for 5 d at room temperature. The solvent was evaporated and the reaction mixture was subjected to a column separation. The pure fractions were collected and the final product was obtained after crystallization from a methanol–CH_2Cl_2 mixture.

1-1*H*,1*H*-Perfluoroheptyl 11-[pentakis(4-methylphenyl-ethynyl)phenoxy]undecanoic acid ester (monomer 2a). Column chromatography using SiO_2 and CH_2Cl_2–hexane (1 : 1 to 3 : 2) as eluent. Yield after crystallization: 59% of a pale yellow powder. ^{1}H NMR (400 MHz, $CDCl_3$): δ = 7.48–7.39, 7.14–7.05 (2 × m, 2 × 10H, CH aromatic); 4.52 [t, ^3J(H,F) = 14 Hz, 2H, CH_2CF_2]; 4.28 [t, ^3J(H,H) = 7 Hz, 2H, CH_2O]; 2.34 [t, ^3J(H,H) = 7 Hz, 2H, CH_2CO_2]; 2.32 (s, 15H, CH_3); 1.86–1.17 (m, 16H, CH_2 aliphatic). ^{13}C NMR: see the analysis of **3a**. ^{19}F NMR (376 MHz, $CDCl_3$): δ = −80.61 [t, ^3J(F,F) = 10 Hz, 3F, CF_3]; −119.40 (m, 2F, CF_2CH_2); −122.01, −122.69, −123.25, −126.00 (4 × m, 8F, CF_2). Elemental analysis for $C_{69}H_{53}F_{13}O_3$: required C 70.16%, H 4.86%; found C 69.94%, H 4.79%. Mass spectral analysis (MALDI-ToF): m/z = 1182.2 (MH^+), 1205.2 ($M + Na^+$), 1221.2 ($M + K^+$), calculated mass for $C_{69}H_{53}F_{13}O_3$ = 1181.2 g mol^{-1}.

1-1*H*,1*H*-Perfluorododecyl 11-[pentakis(4-methyl-phenylethynyl)phenoxy]undecanoic acid ester (monomer 2b). Column chromatography using SiO_2 and CH_2Cl_2–hexane (1 : 1 to

3 : 2) as eluent. Yield after crystallization: 69% of a pale yellow powder. ^{1}H NMR (400 MHz, $CDCl_3$): δ = 7.48–7.39, 7.14–7.05 (2 × m, 2 × 10H, CH aromatic); 4.52 [t, ^3J(H,F) = 14 Hz, 2H, CH_2CF_2]; 4.28 [t, ^3J(H,H) = 7 Hz, 2H, CH_2O]; 2.34 [t, ^3J(H,H) = 7 Hz, 2H, CH_2CO_2]; 2.32 (s, 15H, CH_3); 1.86–1.17 (m, 16H, CH_2 aliphatic). ^{13}C NMR: see the analysis of **3a**. ^{19}F NMR (376 MHz, $CDCl_3$): δ = −80.59 [t, ^3J(F,F) = 10 Hz, 3F, CF_3]; −119.37 (m, 2F, CF_2CH_2); −121.40–(−121.80) (m, 12F, CF_2); −122.53, −123.18, −126.90 (3 × m, 6F, CF_2). Elemental analysis for $C_{74}H_{53}F_{23}O_3$: required C 62.10%, H 4.01%; found C 61.91%, H 3.97%. Mass spectral analysis (MALDI-ToF): *m*/*z* = 1432.3 (MH^+), 1454.3 (M + Na^+); calculated mass for $C_{74}H_{53}F_{23}O_3$ = 1431.2 g mol^{-1}.

1,12-1*H*,1*H*-,12*H*,12*H*-Perfluorododecylene bis{11-[pentakis(4-methylphenylethynyl)phenoxy]undecanoic acid ester} (dimer 3a). Column chromatography using SiO_2 and CH_2Cl_2 hexane (1 : 1) as eluent. Yield after crystallization: 78% of a pale yellow powder. ^{1}H NMR (400 MHz, $CDCl_3$): δ = 7.52–7.45, 7.20–7.13 (2 × m, 2 × 20H, CH aromatic); 4.58 [t, ^3J(H,F) = 14 Hz, 4H, CH_2CF_2]; 4.35 [t, ^3J(H,H) = 7 Hz, 4H, CH_2O]; 2.39 [t, ^3J(H,H) = 7 Hz, 4H, CH_2CO_2]; 2.38 (s, 30H, CH_3); 1.91–1.18 (m, 32H, CH_2 aliphatic). ^{13}C NMR (100 MHz, $CDCl_3$): δ = 172.11 (*o*); 160.25 (*k*); 138.99, 138.86, 138.68 (*b*, *b*′, *b*″); 131.71, 131.59, 131.54 (*c*, *c*′, *c*″); 129.20 (*d*, *d*′, *d*″, convoluted); 128.71 (*i*); 123.99 (*h*); 120.46 (*j*); 120.29, 120.23, 120.06 (*e*, *e*′, *e*″); 99.44, 99.29, 97.17 (*g*, *g*′, *g*″), 87.00, 86.51, 84.01 (*f*, *f*′, *f*″); 74.75 (*l*); 59.21 (*C*H_2CF_2 spacer); 36.63 (*n*); 30.73–25.03 (*m*); 21.59–21.55 (*a*, *a*′, *a*″ convoluted). For ^{13}C assignment, see Scheme 1. Note that the carbon atoms in the perfluorinated chain were not identified due to slow relaxation and CF coupling. ^{19}F NMR (376 MHz, $CDCl_3$): δ −119.38 (m, 4F, CF_2CH_2); −121.59, −121.62, −121.74, −121.18, (4 × m, 16F, CF_2). Elemental analysis for $C_{136}H_{114}F_{20}O_6$: required C 73.44%, H 5.17%; found C 73.62%, H 5.28%. Mass spectral analysis (MALDI-ToF): *m*/*z* = 2225.4 (MH^+), 2247.4 (M + Na^+), 2263.4 (M + K^+); calculated mass for $C_{136}H_{114}F_{20}O_6$ = 2224.3 g mol^{-1}.

1,12-dodecyl bis{11-[pentakis(4-methylphenylethynyl)-phenoxy]undecanoic acid ester} (dimer 3b). Column chromatography using SiO_2 and CH_2Cl_2 hexane (1 : 2 to 2 : 1) as eluent. Yield after crystallization: 46% of a yellow powder. ^{1}H NMR (400 MHz, $CDCl_3$): δ = 7.55–7.48, 7.19–7.12 (2 × m, 2 × 20H, CH aromatic); 4.34 [t, ^3J(H,H) = 7 Hz, 4H, CH_2O]; 4.04 [t, ^3J(H,H) = 7 Hz, 4H, CH_2OCO]; 2.39 [t, ^3J(H,H) = 7 Hz, 4H, CH_2CO_2]; 2.37 (s, 30H, CH_3); 1.95–1.20 (m, 52H, CH_2 aliphatic). ^{13}C NMR (100 MHz, $CDCl_3$): δ = 174.00 (*o*); 160.24 (*k*); 138.99, 138.86, 138.67 (*b*, *b*′, *b*″); 131.71, 131.59, 131.54 (*c*, *c*′, *c*″); 129.20, 129.18, 129.16 (*d*, *d*′, *d*″); 128.71 (*i*); 123.01 (*h*); 120.47 (*j*); 120.30, 120.24, 120.08 (*e*, *e*′, *e*″); 99.44, 99.30, 97.21 (*g*, *g*′, *g*″), 87.01, 86.53, 84.02 (*f*, *f*′, *f*″); 74.76 (*l*); 64.39 (*C*H_2OCO spacer); 34.29 (*n*); 30.57–25.03 (*m* and CH_2 spacer); 21.59–21.56 (*a*, *a*′, *a*″ convoluted). For ^{13}C assignment, see Scheme 1. Elemental analysis for $C_{136}H_{134}O_6$: required C 87.61%, H 7.24%; found C 87.72%, H 7.42%. Mass spectral analysis (MALDI-ToF): *m*/*z* = 1865.6 (MH^+), 1887.6 (M + Na^+), 1903.6 (M + K^+); calculated mass for $C_{136}H_{134}O_6$ = 1864.5 g mol^{-1}.

Mixtures. An equimolar mixture of **3a** and **3b** was prepared by dissolving the appropriate amounts of the dimers in CH_2Cl_2, evaporation of the solvent and drying overnight in vacuum.

Acknowledgements

The authors thank the Ramsay Memorial Fellowship Trust and the EU (RTN "LCDD" contract HPRN-CT2000-00016) for financial support.

References

1 (*a*) A. J. Leadbetter, *The Molecular Physics of Liquid Crystals*, ed. G. R. Luckhurst and G. W. Gray, Academic Press, London 1979, p. 285; (*b*) A. J. Leadbetter and R. M. Richardson, *The Molecular Physics of Liquid Crystals*, ed. G. R. Luckhurst and G. W. Gray, Academic Press, London, 1979, p. 451; (*c*) P. Davidson, D. Petermann and A. M. Levelut, *J. Phys. II*, 1995, **5**, 113; (*d*) G. Ungar, *Liquid Crystal Nematics*, ed. D. A. Dunmur, A. Fukuda, G. R. Luckhurst, Inspec, London, 2001, pp 177.

2 (*a*) A. M. Donald and A. H. Windle, *Liquid Crystalline Polymers*, Cambridge University Press, Cambridge, UK, 1992; (*b*) O. Francescangeli, M. Laus and G. Galli, *Phys. Rev. E*, 1997, **55**, 481; (*c*) V. Percec, P. Chu, G. Ungar and J. Zhou, *J. Am. Chem. Soc.*, 1995, **117**, 11441; (*d*) S. Haddawi, S. Diele, H. Kresse, G. Pelzl, W. Weissflog and A. Wiegeleben, *Liq. Cryst.*, 1994, **17**, 191; (*e*) S. Stojadinovic, A. Adorjan, S. Sprunt, H. Sawade and A. Jakli, *Phys. Rev. E*, 2002, **66**, 060701.

3 (*a*) L. A. Madsen, T. J. Dingemans, M. Nakata and E. T. Samulski, *Phys. Rev. Lett.*, 2004, **92**, 145505; (*b*) B. A. Acharya, A. Primak and S. Kumar, *Phys. Rev. Lett.*, 2004, **92**, 145506.

4 (*a*) A. de Vries, *Mol. Cryst. Liq. Cryst.*, 1970, **10**, 219; (*b*) J. Als-Nielsen, R. J. Birgeneau, J. D. Litster and C. R. Safiniya, *Phys. Rev. Lett.*, 1977, **39**, 352; (*c*) L. J. Martinez-Miranda, A. R. Kortan and R. J. Birgeneau, *Phys. Rev. Lett.*, 1986, **56**, 2264; (*d*) R. J. Birgeneau, C. W. Garland, G. B. Casting and B. M. Ocko, *Phys. Rev. A*, 1981, **24**, 2624; (*e*) K. W. Evanslutterodt, J. W. Chung, B. M. Ocko and R. J. Birgeneau, *Phys. Rev. A*, 1987, **36**, 1387.

5 For reviews on discotic liquid crystals, read: (*a*) K. Praefcke, *Liquid Crystal Nematics*, ed. D. A. Dunmur, A. Fukuda, G. R. Luckhurst, Inspec, London, 2001, p. 17; (*b*) N. Boden and B. Movaghar, *Handbook of Liquid Crystals,*, ed. D. Demus, J. W. Goodby, G. W. Gray, H. W. Spiess and V. Vill, Wiley VCH, New York, 1998, vol. 2B, p. 781; (*c*) R. J. Bushby and O. W. Lozman, *Curr. Opin. Colloid Interface Sci.*, 2002, **7**, 343; (*d*) S. Kumar, *Chem. Soc. Rev.*, 2006, **35**, 83.

6 (*a*) B. Alameddine, O. F. Aebischer, W. Amerin, B. Donnio, R. Deschenaux, D. Guillon, C. Savary, D. Scanu, O. Scheidegger and T. A. Jenny, *Chem. Mater.*, 2005, **17**, 4798; (*b*) Y. Xu, S. Leng, C. Xue, R. Sun, J. Pan, J. Ford and S. Jin, *Angew. Chem., Int. Ed.*, 2007, **46**, 3896.

7 (*a*) P. H. J. Kouwer and G. H. Mehl, *Angew. Chem., Int. Ed.*, 2003, **42**, 6015; (*b*) P. H. J. Kouwer, J. Pourzand and G. H. Mehl, *Chem. Commun.*, 2004, 66; (*c*) Y. Shimizu, A. Hurobe, H. Monobe, N. Terasawa, K. Kiyohara and K. Uchida, *Chem. Commun.*, 2003, 1676 (meta-stable smectic phase).

8 (*a*) P. Marczuk and P. Lang, *Macromolecules*, 1998, **31**, 9013; (*b*) J. Höpken, C. Pugh, W. Richtering and M. Möller, *Makromol. Chem.*, 1988, **189**, 911; (*c*) R. J. Twieg, T. P. Russell, R. L. Siemens and J. F. Rabolt, *Macromolecules*, 1985, **18**, 1361; (*d*) J. F. Rabolt, T. P. Russell and R. J. Twieg, *Macromolecules*, 1984, **17**, 2786; (*e*) L. M. Blinov, T. A. Lobko, B. I. Ostrovkii, S. N. Sulianov and F. G. Tournilhac, *J. Phys. II*, 1993, **3**, 1121; (*f*) S. Pensec, F. G. Tournilhac, P. Bassoul and C. Durliat, *J. Phys. Chem. B*, 1998, **102**, 52; (*g*) F. Guittard, E. T. de Gevinchy, S. Geribaldy and A. Cambon, *J. Fluorine Chem.*, 1999, **100**, 85.

9 (*a*) H. T. Nguyen, G. Sigaud, M. F. Achard, F. Hardouin, R. J. Tweig and K. Betterton, *Liq. Cryst.*, 1991, **10**, 389; (*b*) Y. H. Chiang, A. E. Ames, R. A. Guandiana and T. G. Adams, *Mol. Cryst. Liq. Cryst.*, 1991, **208**, 85; (*c*) M. Ibn-Elhaj, H. J. Coles, D. Guillon and A. Skoulios, *J. Phys. II*, 1993, **3**, 1807; (*d*)

K. J. Shepperson, T. Meyer and G. H. Mehl, *Mol. Cryst. Liq. Cryst.*, 2004, **411**, 185; (*e*) G. H. Mehl and J. W. Goodby, *Chem. Ber.*, 1996, **129**, 521; (*f*) G. H. Mehl and J. W. Goodby, *Angew. Chem., Int. Ed. Engl.*, 1996, **35**, 2641.

10 (*a*) H. Yoshizawa, T. Mihara and N. Koide, *Mol. Cryst. Liq. Cryst.*, 2004, **423**, 61; (*b*) D. Navarro-Rodriguez, Y. Frere, P. Gramain, D. Guillon and A. Skoulios, *Liq. Cryst.*, 1991, **9**, 321; (*c*) L. Cui, V. Sapagovas and G. Lattermann, *Liq. Cryst.*, 2002, **29**, 1121.

11 Stabilised columnar phases by the use of one or multiple fluorinated tails: (*a*) U. Dahn, C. Erdelen, H. Ringsdorf, R. Festag, J. H. Wendorff, P. A. Heiney and N. C. Maliszewsky, *Liq. Cryst.*, 1995, **19**, 759–764; (*b*) Stabilisation of the columnar phase after introduction of terminal siloxane groups: R. Zniber, R. Achour, M. Z. Cherkaoui, B. Donnio, L. Gehringer and D. Guillon, *J. Mater. Chem.*, 2002, **12**, 2208; (*c*) Stabilisation of the columnar phase after introduction of terminal siloxane groups: J. Motoyanagi, T. Fukushima and T. Aida, *Chem. Commun.*, 2005, 101.

12 P. H. J. Kouwer, G. H. Mehl and S. J. Picken, *Mol. Cryst. Liq. Cryst.*, 2004, **411**, 387.

13 The rigid mesogen fraction (M) is defined as the weight fraction of aromatic groups in the mesogen. Because of its limited positional flexibility, the lateral methyl group is included in the rigid part of the mesogen as well.

14 (*a*) P. H. J. Kouwer, W. J. Mijs, W. F. Jager and S. J. Picken, *J. Am. Chem. Soc.*, 2001, **123**, 4645; (*b*) P. H. J. Kouwer, J. Gast, W. F. Jager, W. J. Mijs and S. J. Picken, *Mol. Cryst. Liq. Cryst.*, 2001, **364**, 225.

15 (*a*) P. H. J. Kouwer and G. H. Mehl, *J. Am. Chem. Soc.*, 2003, **125**, 11172; (*b*) P. H. J. Kouwer and G. H. Mehl, *Mol. Cryst. Liq. Cryst.*, 2003, **397**, 301.

16 The small decrease in the lateral disc–disc distance indicated by reflection B of all fluorinated materials with respect to the alkylated materials can be explained by considering that of the (fluorinated) discs, the terminal end of the tail is anchored. This imposes a restricted rotation around the short axis of the mesogen, which—in turn—results in a smaller lateral distance.